

# Electronic Supplementary Information (ESI)

## Statistical analysis of discrete encapsulation of nanomaterials in colloidal capsules

*Tatsuya Sakakura,<sup>1</sup> Kazuya Nishimura,<sup>1</sup> Hiroaki Suzuki,<sup>1,2</sup> Tetsuya Yomo<sup>1, 2, 3, \*</sup>*

<sup>1</sup> Department of Bioinformatic Engineering, Graduate School of Information Science and Technology, Osaka University, Yamadaoka 1-5, Suita, Osaka 565-0871, Japan; <sup>2</sup> Exploratory Research for Advanced Technology (ERATO), Japan Science and Technology Agency, Yamadaoka 1-5, Suita, Osaka 565-0871; <sup>3</sup> Department of Frontier Biosciences, Graduate School of Frontier Biosciences, Osaka University, Yamadaoka 1-5, Suita, Osaka 565-0871, Japan.

### Contents:

1. Supplementary Information Text
  - Concentration of the volume marker in vesicles
  - Confirmation of the conversion factor
2. Supplementary Figures
  - Fig. S1. Confocal fluorescence images of vesicles.
  - Fig. S2. Calibration curve (F.I. vs A647 molecules).
  - Fig. S3. Size distributions of vesicles.
  - Fig. S4. Concentration of YG beads vs dilution.
  - Fig. S5. Concentration of  $\lambda$ DNA vs dilution.
  - Fig. S6.  $P_k(V)$  vs  $V$  curves for vesicles (natural swelling and W/O transfer methods)
  - Fig. S7. Example of 2D density plot for  $\lambda$ DNA encapsulation
  - Fig. S8.  $P_k(V)$  vs  $V$  curves for vesicles (neutral, negative and positive vesicles)

## 1. Supplementary Information Text

**Concentration of the volume marker in vesicles:** To convert the number of APC molecules to the vesicle volume, the concentration in the vesicles has to be known. Although we confirmed in our previous studies that the APC concentration in vesicles are the same as that in the bulk concentration (500 nM), we re-confirmed this fact again in this study because the vesicle volume is a critical factor in evaluating the encapsulation phenomena. To do this we observed vesicles under a confocal fluorescent microscope (CSU-X1, Yokogawa Electric). The 500 nM of APC was supplemented in the outer solution, so that the APC concentrations in and out of vesicles should become the same. As seen in Fig. S1, fluorescence intensities from APC inside and outside of vesicles are the same, indicating that the APC concentration in vesicles is 500 nM as we designed.

**Confirmation of the conversion factor:** We further performed an experiment to double-check the credibility of the vesicle volume evaluation. That is, we prepared the liposome population having uniform volumes, and compared the volume distribution derived from the microscope images and the F. I. distribution derived from the FCM measurement. We prepared liposomes with the W/O emulsion transfer method with the lipid composition POPC:POPG:Chol = 9:1:1 (weight ratio). Then, we extruded this liposome suspension through the polycarbonate membrane with a syringe and a membrane holder (SH13, GE Healthcare) to reduce the vesicles larger than the pore size. Followingly, the extruded vesicles were subjected to dialysis to remove vesicles smaller than the dialysis pore size. We prepared two vesicle populations with this protocol; the first population (P1) was extruded through 10  $\mu\text{m}$  pore and dialyzed with 5  $\mu\text{m}$  pore for 216 h. The second

population (P2) was extruded through 5  $\mu\text{m}$  pore and dialyzed with 3  $\mu\text{m}$  pore for 160 h.

We first measured the volume marker F.I. distribution of these vesicles by the FACS, which is shown in Fig. S3.

Note that, in the FACS measurement results (a1; P1 population and a2; P2 population), the peak values for F.I.

shifted to the larger values after dialysis. We fitted these peaks with the Gaussian distribution in logarithm

scale (red solid lines) to obtain the most frequent value ( $2.2 \times 10^5$  and  $4.2 \times 10^4$ , respectively). Then we derived

the volume distribution of the identical vesicle populations from the microscope image analysis. Diameters of

more than 300 vesicles were measured, from which volume was calculated based on the diameter. The final

histograms are shown in Fig. S3 (a2; P1 population) and (b2; P2 population). The peak values of the volume

distributions are 178 and 37 fL, respectively. Therefore, the conversion factors from this analysis yield 0.0082

and 0.0088, respectively. These values are in good agreement with the conversion factor derived from the

fluorescent-bead calibration. This experiment confirmed that encapsulation of the volume marker is ideal, and

volume evaluation from the FACS measurement is reliable.

## 2. Supplementary Figures

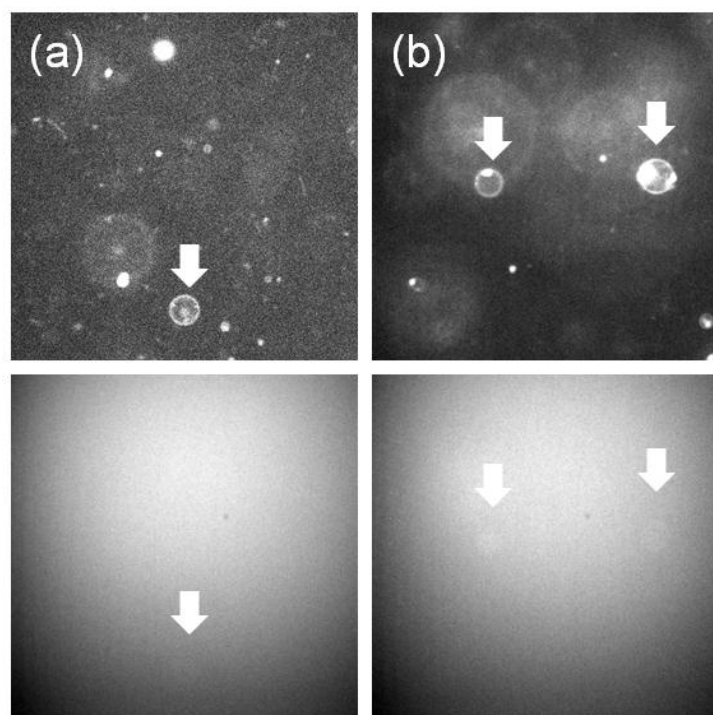


Fig. S1. Confocal fluorescence images of vesicles. (a) Vesicles formed by the natural swelling method. (b) Vesicles formed by the W/O emulsion transfer method. The upper images show the membrane (emission from the membrane marker,  $\beta$ -BODIPY-HPC) and the lower images show the emission from the volume marker, APC. It is obvious that the emission from the volume marker inside vesicles exhibits the same intensity as that of the outside solution. This result shows that the APC concentration in vesicles is 500 nM as we designed.

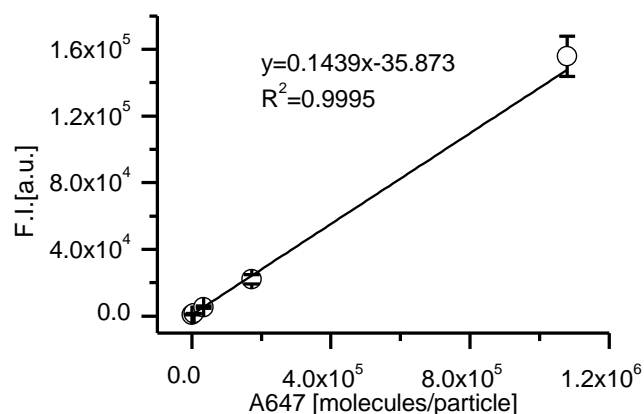


Fig. S2. Calibration curve that relates the number of fluorescent molecules per a particle and fluorescence intensity detected by FCM. Error bars represent the standard deviation of the measured fluorescent intensities (F.I.) of the calibration beads.

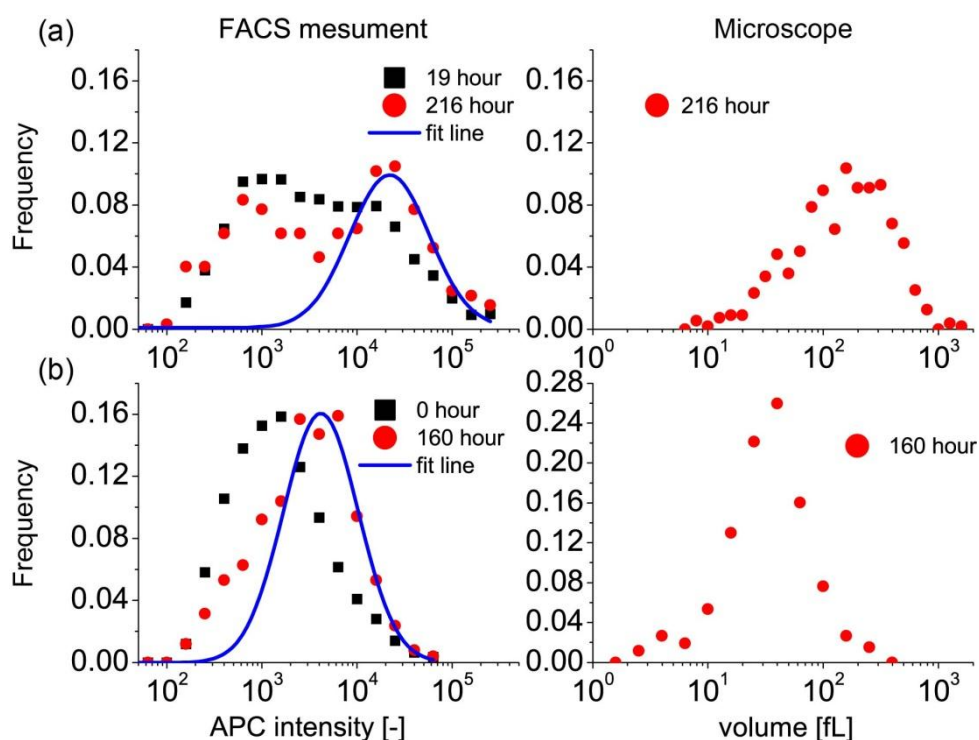


Fig. S3. Size (Volume) distributions of vesicles after size separation. Volume was measured by FACS and microscope image analysis for comparison. (a) Volume distributions of P1 vesicles. (b) Volume distributions of P2 vesicles. Left and right figures show the distributions derived from FACS and microscope image analyses, respectively.

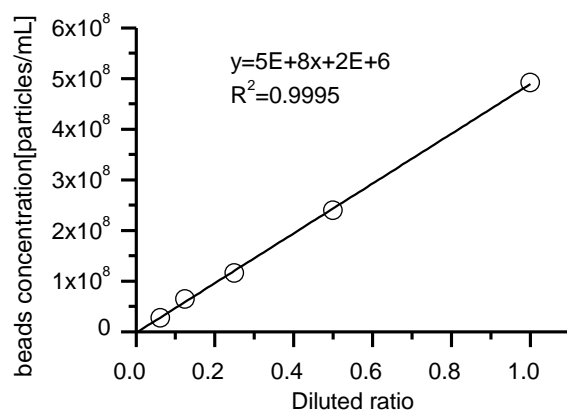


Fig. S4. Dilution of 0.35  $\mu\text{m}$  YG beads and its absolute concentration.

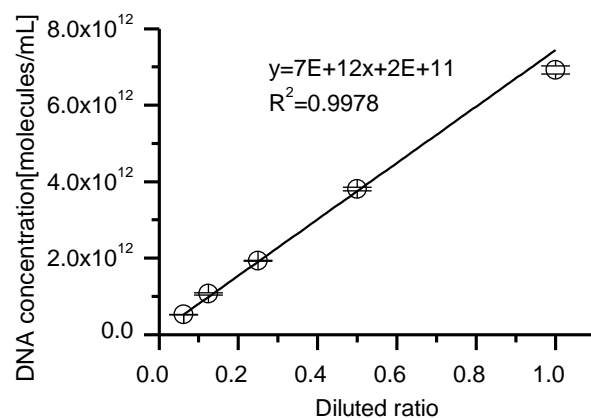
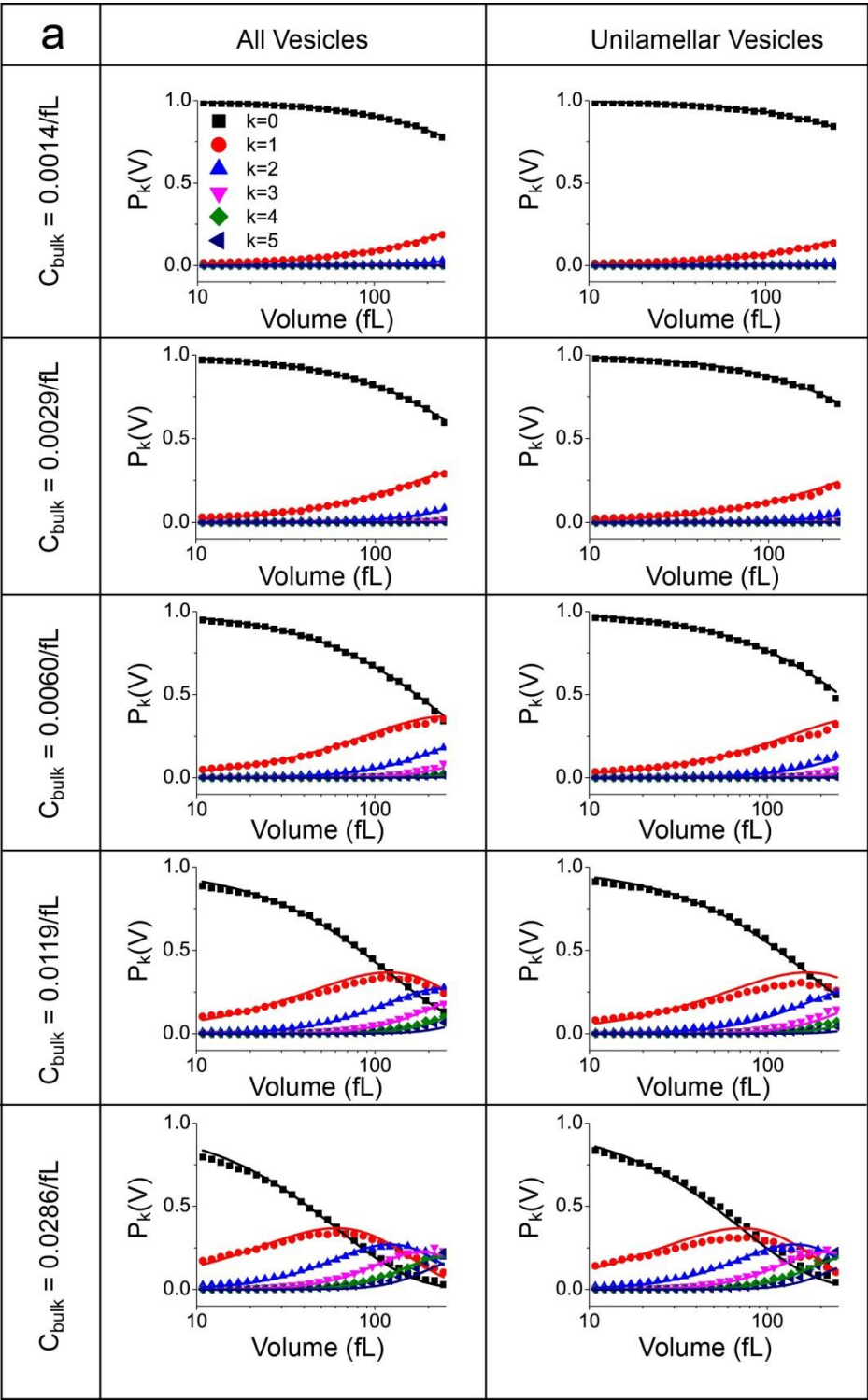


Fig. S5. Dilution of  $\lambda$ DNA and its concentration measured by the UV absorbance. Error bar represents the standard deviation of five measurements.



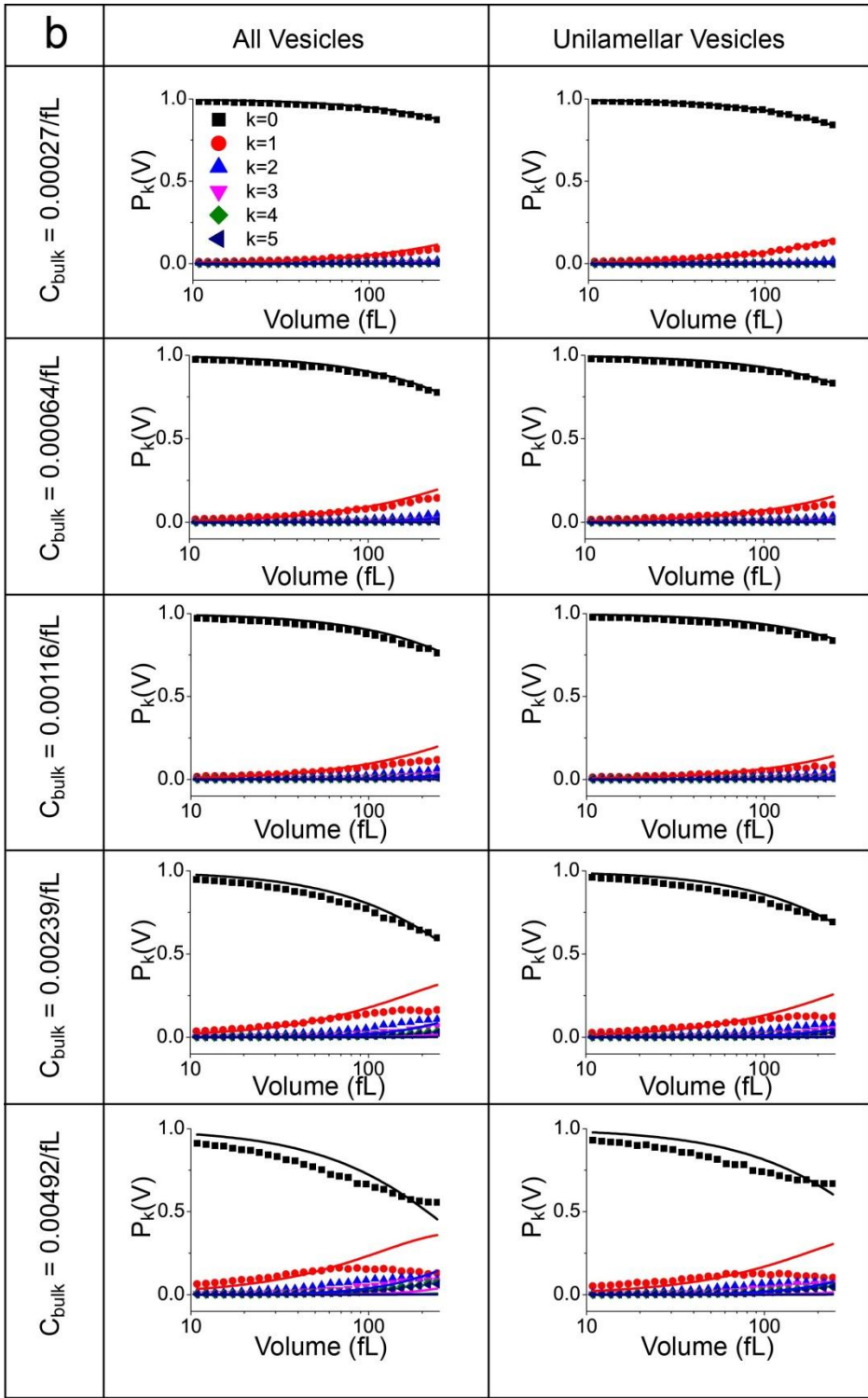


Fig. S6. Volume dependence of the probability of vesicles enclosing  $k$  beads ( $P_k(V)$ ;  $k = 0, 1, 2, 3, 4$ , and  $5$ ). (a) Natural swelling method and (b) W/O emulsion transfer method. Results for all  $C_{\text{bulk}}$  studied are shown. Statistics for all vesicles and for nearly unilamellar vesicles are shown in the left and right columns, respectively. Solid lines show the global fitting curves of Poisson distribution (Eq. 3) with the single parameter  $\lambda$ .



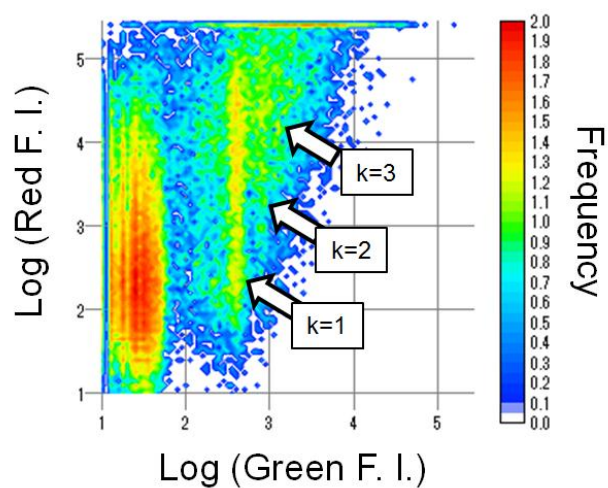
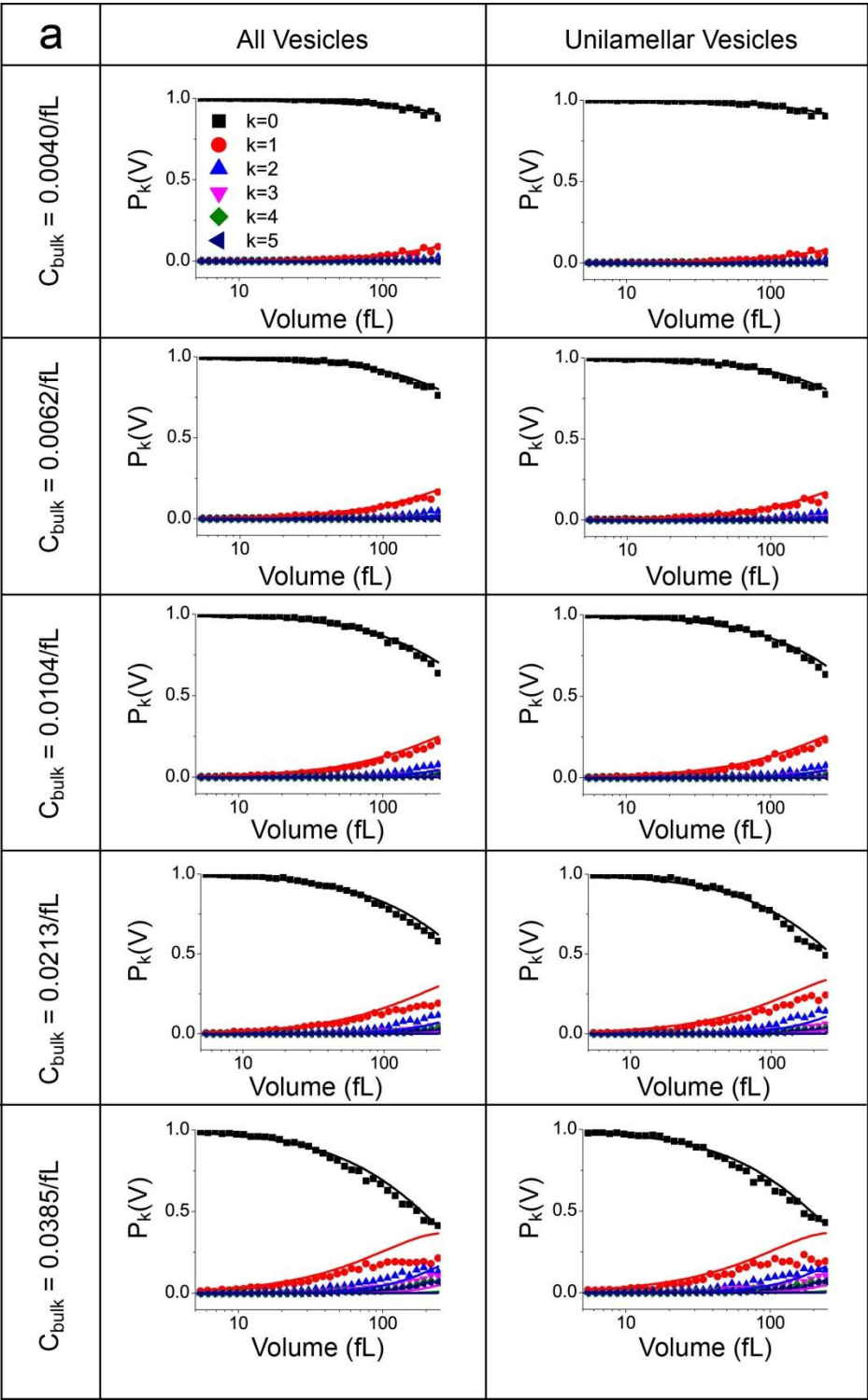
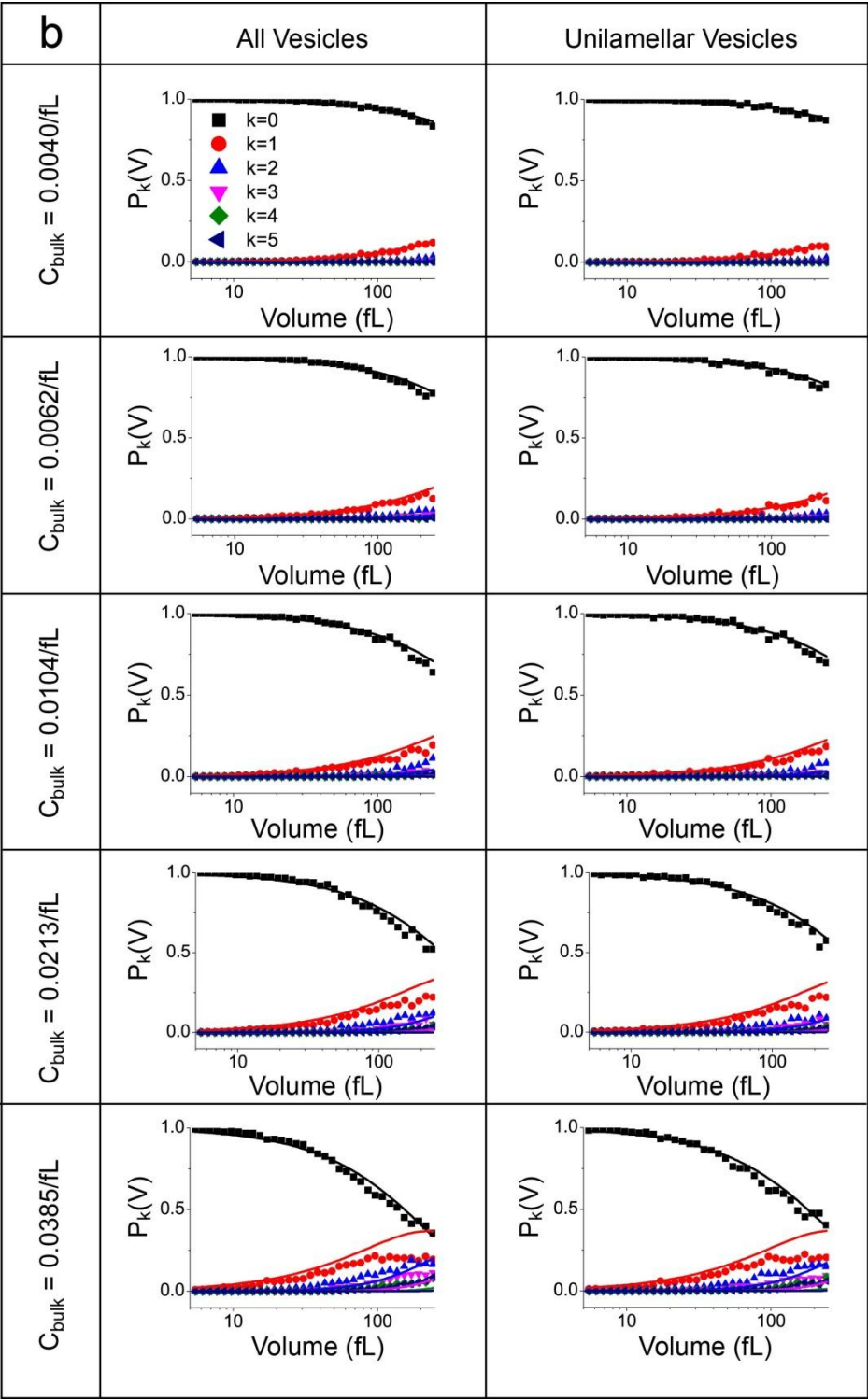


Fig. S7. Example of the raw data for the measurement of vesicle population encapsulating  $\lambda$ DNA. Measurement result for positively charged vesicles prepared at  $C_{\text{bulk}} = 0.0172$  /fL is shown. Number of  $\lambda$ DNA in vesicles is quantized.





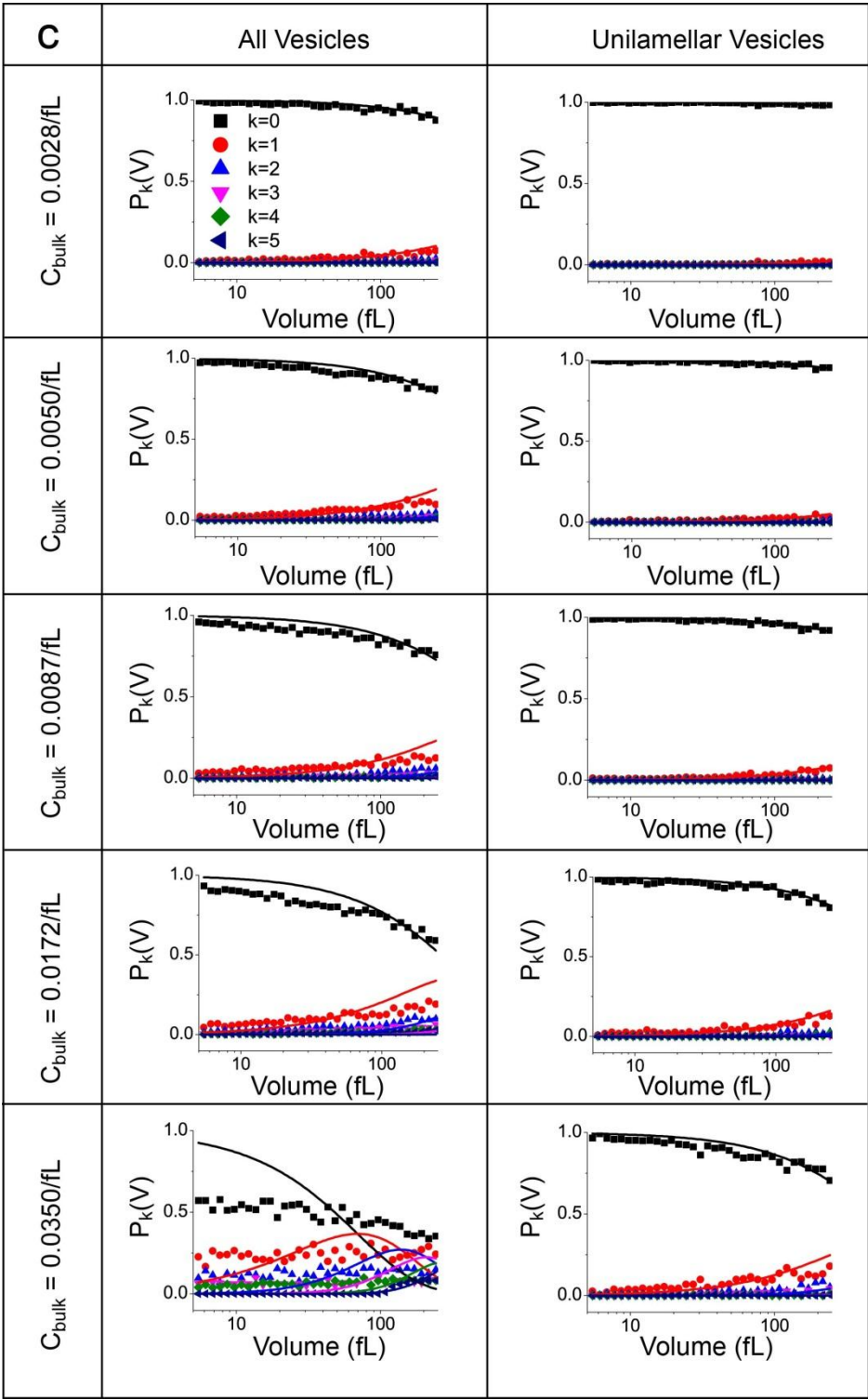


Fig. S8. Volume dependence of the probability of vesicles enclosing  $k$  beads ( $P_k(V)$ ;  $k = 0, 1, 2, 3, 4$ , and  $5$ ). All vesicles are prepared by the W/O emulsion transfer method. (a) Neutral vesicles. (b) Negatively charged vesicles. (c) Positively charged vesicles. Results for all  $C_{\text{bulk}}$  studied are shown. Statistics for all vesicles and for nearly unilamellar vesicles are shown in the left and right columns, respectively. Solid lines show the global fitting curves of Poisson distribution (Eq. 3) with the single parameter  $\lambda$ .